



## **Fabrication of counter electrode for dye sensitized solar cells application using environmentally friendly graphene and carbon nanotubes composite materials**

**Fatiatun Fatiatun<sup>\*</sup>, Nugroho Prasetya Adi**

*Department of Physics Education, Universitas Sains Al-Qur'an, Indonesia*

*\*E-mail: [fatia@unsiq.ac.id](mailto:fatia@unsiq.ac.id)*

(Received: 29 July 2021; Accepted: 05 April 2022; Published: 07 April 2022)

### **ABSTRACT**

In this research, carbon nanotubes (CNTs) was composited with graphene for *counter electrode* (CE) in dye sensitized solar cells (DSSCs) application. CNTs used were derivated from waste of palm oil that were environmentally friendly. The composited graphene and CNTs were fabricated on *fluorine tin oxide* (FTO) substrates by spray coating method. The aims in this study to improve electrical conductivity of CE which graphene hybridized with CNTs. Graphene oxide (GO) with home-made triple-tails sodium 1,4-bis(neopentyloxy)-3-(neopentyloxycarbonyl)-1,4-dioxobutane-2-silphonate (TC14) surfactant (TC14-GO), reduced GO (TC14-rGO) and hybrid of TC14-rGO with CNTs (TC14 rGO-CNTs hybrid) were fabricated for CE in DSSCs application. Based on four-point probe measurement, the TC14 rGO-CNTs hybrid presented high electrical conductivity of  $\sim 6.8 \times 10^{-1} \text{ S.cm}^{-1}$ . This consistent with solar simulator result that TC14 rGO-CNTs hybrid as CE sample showed high efficiency of 0.0132%.

**Keywords :** *carbon nanotubes, counter electrode, dye sensitized solar cells, graphene*

DOI: [10.30870/gravity.v8i1.12028](https://doi.org/10.30870/gravity.v8i1.12028)

### **INTRODUCTION**

Solar cells have been widely developed in the world because of the limited amount of fossil materials in nature that are usually used to generate electricity. Dye sensitized solar cells-DSSCs are part of the solar cells that have developed at this time and are used as an alternative to silicon-based solar cells (Chadijah et al., 2016). Silicon-based solar cells are

included in the inefficient category because they consume very high costs for production (Ichikawa et al., 2001). In solar cells, sunlight is used as an energy source which is then converted into electrical energy. Indonesia is a tropical country that always gets maximum sunlight. Based on Indonesia is a tropical country, solar cells are very suitable to be applied in Indonesia which gets a lot of sunlight.

DSSCs receive high attention in the world because of their lower production costs and relatively easy manufacturing process (Fatiatun et al., 2020). DSSCs have 4 important components, all of which affect the final efficiency results which are known by measurement. These components are photo-anode, dye-sensitizer, electrolyte and counter electrode (CE). One of the important components in DSSCs is CE which acts as a catalyst in the reduction reaction of triiodide ions ( $I_3^-$ ) to iodide ions ( $I^-$ ) (Gratzel, 2003). In converting solar energy into electrical energy, the reduction process in CE plays a very important role in determining whether the process is fast or slow (Chadijah et al., 2016).

Platinum (Pt) is a very common material used for CE fabrication because of its stability to  $I_3^-/I^-$  electrolytes and also high catalyst activity (Wu et al., 2014). However, Pt is expensive and the quantity is limited in nature, so it is necessary to develop other materials to reduce or replace Pt in CE fabrication (Choi et al., 2011; Yang Z et al., 2011). Carbon is a material that has received a lot of attention from researchers to be developed as a replacement for Pt in CE fabrication. In the previous study, carbon showed high efficiency of 16.2% in DSSCs application (Liu et al., 2019). In recent years, the development of research on carbon is very high because of its low price and abundant availability in nature.

The carbon family that has been widely developed for CE materials in the application of DSSCs is graphene which has high electrical conductivity and stability. There are several derivative materials from graphene that have been developed several years ago, namely graphene oxide (GO). GO was produced using the electrochemical exfoliation method (Suriani et al., 2018). The synthesized GO then reduced the oxygen content in the solution by a reduction process to produce a reduced graphene oxide (rGO) solution with a smaller amount of oxygen. The low oxygen content of rGO makes it more conductive, has a better and more stable structure (Suriani et al., 2019). Based on this, researchers will develop rGO as a material in the fabrication of CE which is composited with carbon nanotubes (CNTs) derived from palm oil waste. This composite between rGO and CNTs aims to complement each other properties to create better and environmentally friendly properties for CE in the application of DSSCs.

## **RESEARCH METHODS**

### **Synthesis of Graphene Oxide**

Electrochemical exfoliation method was used to synthesis of GO which done in an electrolyte containing surfactants. Home-made triple-tail TC14 surfactants and commercially available single-tail sodium dodecyl sulphate (SDS) were utilized in GO synthesis with an electrolyte content of 0.1 M. Two graphite rods used in the synthesis of GO which were immersed in an electrolyte solution and connected to a potential of 7V at room temperature

for 24 hours. Electrolytes are made by mixing surfactants with deionized water (DI-water).

### **Production of Reduced Graphene Oxide**

In rGO production by reduction process, the GO solution that has been successfully synthesized is then reduced of oxygen content. Hydrazine hydrate is used as an reducing agent in the reduction process with ratio 1:100 (hydrazine hydrate:GO solution) and the reduction process was done at  $\sim 95^{\circ}\text{C}$  for 24 hours. Figure 1 shows the detail processing of rGO production.

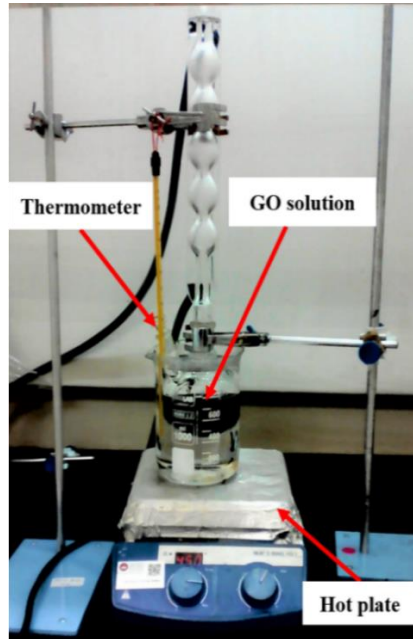


**Figure 1.** Production of reduced graphene oxide

### **Composite of Reduced Graphene Oxide and Carbon Nanotubes**

The TC14 rGO/CNTs hybrid was prepared by mixing CNTs powder and TC14-rGO solution. Furthermore, the composite solution of TC14-rGO and CNTs (TC14 rGO/CNTs hybrid) was stirred for 1 hour on a hot plate with a magnetic stirrer and sonicated for 30 minutes at room temperature.

### **Transfer Process of TC14-GO, TC14-rGO and TC14 rGO-CNTs hybrid**

Before the transfer process, FTO glass substrate was cleaned with an ultrasonic cleaner using acetone, methanol and DI-water. The cleaned glass substrate was then heated on a hot plate at  $120^{\circ}\text{C}$  for 5 minutes. After that, the spray coating method was utilized to transfer all samples (TC14-GO, TC14-rGO and TC14 rGO/CNTs hybrid) solution on the FTO substrate. Spraying is carried out at a distance of 10 cm from the substrate position. The fabricated thin films were then annealed for 1 hour at  $400^{\circ}\text{C}$  in Ar flow. Figure 2 demonstrates the transfer process of TC14-GO, TC14-rGO and TC14 rGO/CNTs hybrid on FTO substrates by spray coating method.

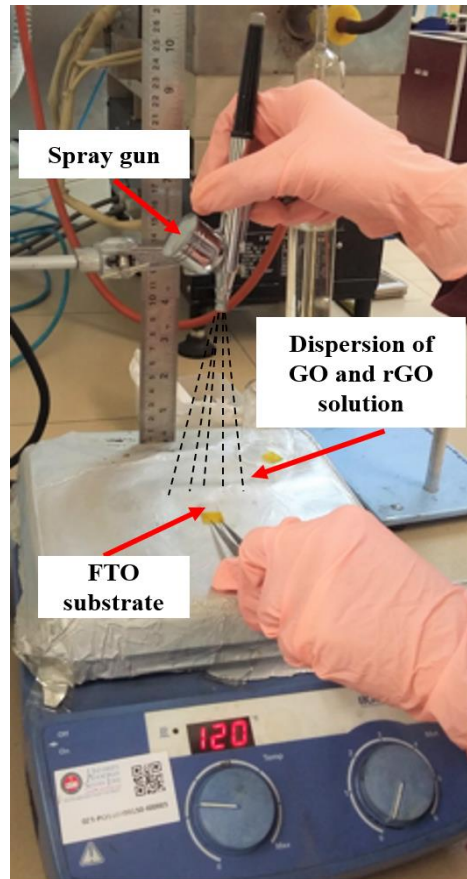


**Figure 2.** The samples sprayed on the FTO substrates via Spray Coating Method

CE thin-film samples were characterized in structural and electrical. The CE structure was characterized using field emission scanning electron microscopy (FESEM), energy dispersive X-ray (EDX), and micro-Raman spectroscopy. Four-point probe (Keithley 2636A) measurements to determine the electrical properties of the CE thin film. The last measurement was carried out using a solar simulator to determine the efficiency of the DSSCs application that has been made by utilizing all the CE samples, namely TC14-GO, TC14-rGO, and TC14 rGO-CNTs hybrid with ZnO/TiO<sub>2</sub> hybrid as photoanode (Sulhadi et al, 2015; Putut M et al., 2016; Fatiatun et al., 2017; Ameer A.A. et al., 2019; Idris NJ et al., 2019), N719 dye and iodide-tri-iodide ( $I/I^{3-}$ ) as electrolyte.

RESULTS AND DISCUSSION

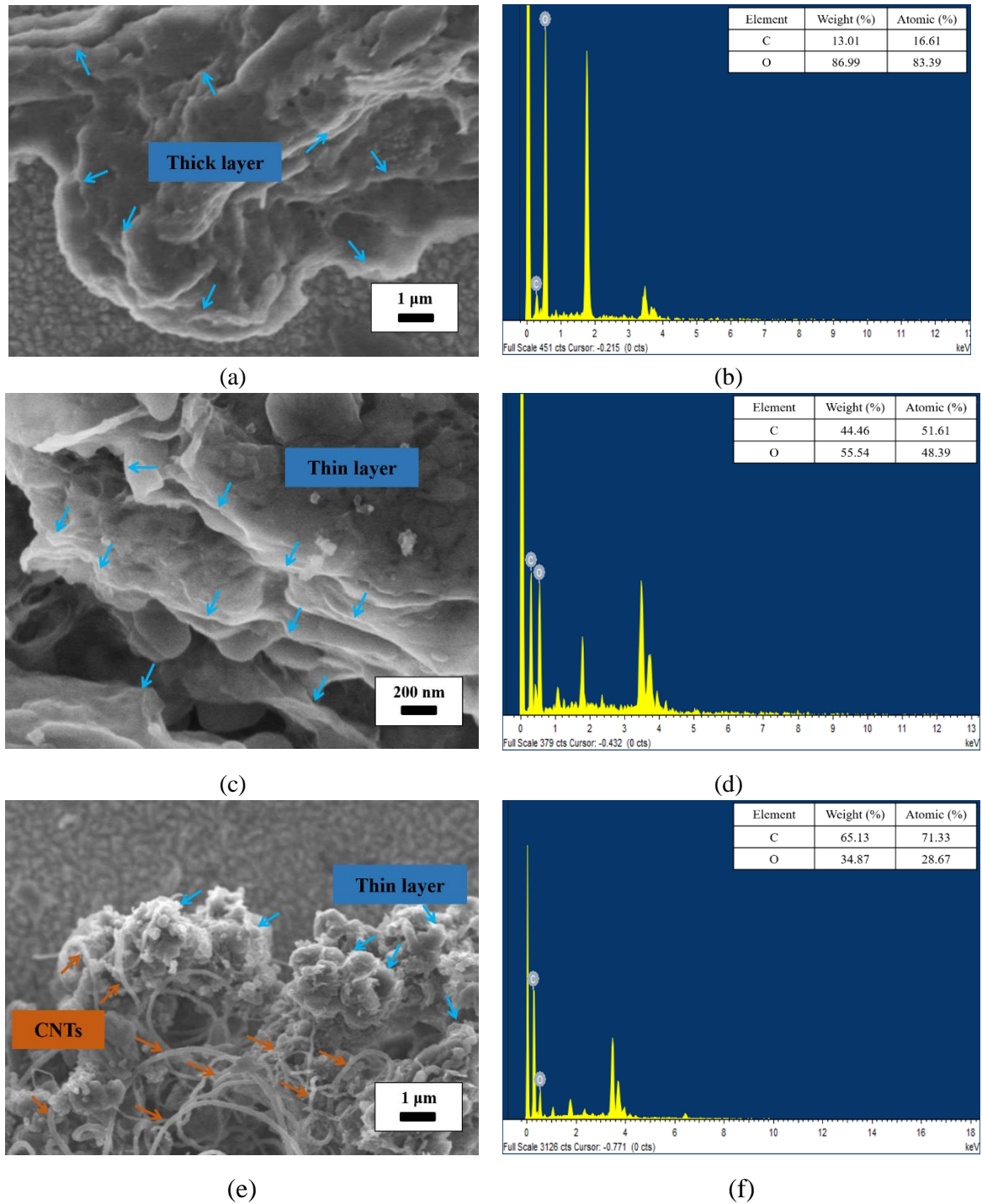


**Figure 3.** Images of FESEM and EDX analysis (a)-(b) TC14-GO, (c)-(d) TC14-rGO, and (e)-(f) TC14 rGO-CNTs hybrid

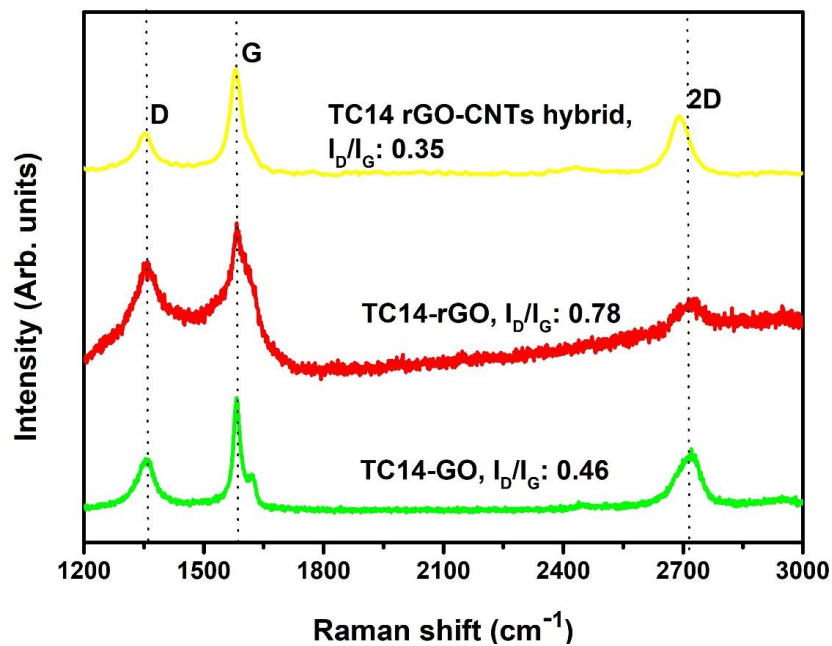
**Figure 3** show the FESEM images of fabricated samples. The GO-TC14 (Figure 3(a)) presented the thick layers and its surface demonstrated wrinkle structure. This structure revealed high oxygen (O) content that produced during oxidation process. Successfully oxidation process proved by EDX analysis that O content (83.39%) presented higher than

Copyright © 2022, Gravity, ISSN 2528-1976

carbon (C) (16.61%) as demonstrated in Fig. 1(b).

The TC14-rGO (Figure 3(c)) presents sheet and thinner layer than TC14-GO. This was believed due to low oxygen content of TC14-rGO which proved successfully reduction process. Based on the EDX analysis (Figure 3(d)), the TC14-rGO showed higher atomic percentage of C (51.61%) than O (4.39%). This result also explained that TC14-rGO presented higher atomic percentage of C than TC14-GO. Therefore, TC14-rGO demonstrated thinner layer and better structure as compared to TC14-GO (Suriani et al., 2018).

The FESEM image of composite of TC14-rGO with CNTs (TC14 rGO-CNTs hybrid) as presented in Figure 3(e)). The morphology structure of TC14-rGO composited with CNTs showed the well-dispersed and scattered TC14-rGO/CNTs on the FTO surface. The vacancies between TC14-rGO layers were filled by CNTs that looked as conjugated network. The CNTs can be also used as connecting wire between TC14-rGO layers (Suriani et al., 2019). The EDX analysis of TC14 rGO-CNTs hybrid (Figure 3(f)) revealed high atomic percentage of C (71.33%). This composite showed higher C (71.33%) content than pristine TC14-rGO (51.61%).



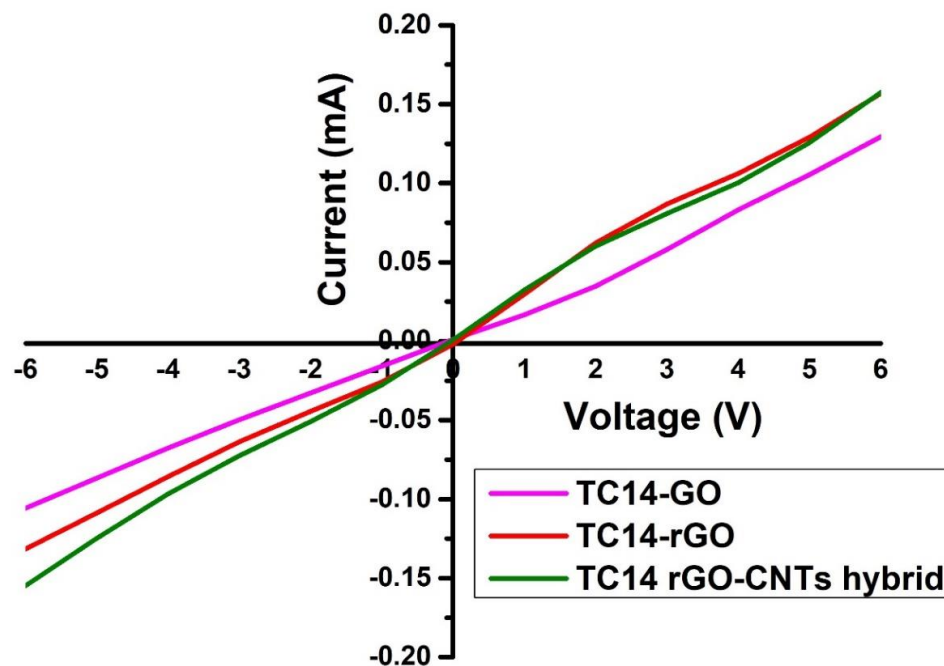
**Figure 4.** Micro-Raman spectra of TC14-GO, TC14-rGO and TC14 rGO-CNTs hybrid

Figure 4 demonstrates the micro-Raman spectra of CE thin film samples. The crystallinity and disorder of thin film samples can be investigated by using this analysis (Ahmed et al., 2011; Surini et al., 2018). The D- and G- bands of TC14-GO are 1354 and 1584  $\text{cm}^{-1}$ , respectively. The D-band shows dangling bonds which indicates the defects in carbon lattice and was known as vibrations of  $\text{sp}^3$  carbon atoms (Yadav et al., 2017).

The G-band can be used to detect the vibrations of  $\text{sp}^2$ -bonded carbon atoms (Chen et al., 2015). Meanwhile, the D- and G- bands of TC14-rGO are 1363 and 1585  $\text{cm}^{-1}$ , respectively. This presents a shifted peak from D- and G-band peak of TC14-GO of 1355 and 1583  $\text{cm}^{-1}$ ,

respectively that indicates successful reduction process. The TC14-rGO/CNTs hybrid shows narrow D- and G-band of 55.04 and 39.60  $\text{cm}^{-1}$ , respectively which were also believed due to narrow D- and G-band of pristine CNTs. TC14 rGO-CNTs hybrid also demonstrates a shifting of D- ( $1351 \text{ cm}^{-1}$ ) and G-bands ( $1580 \text{ cm}^{-1}$ ) to a lower wavelength than those of pristine TC14-rGO ( $1363$  and  $1585 \text{ cm}^{-1}$ , respectively).

From micro-Raman spectra, the  $I_D/I_G$  ratio can be also calculated. The highest  $I_D/I_G$  ratio of 0.78 was shown by TC14-rGO. This higher than TC14-GO of 0.46 because of the decrement of oxygen content in part of restoration the  $\pi$ -conjugated systems and distortion of graphitic domains during the reduction process (Samad et al., 2016). Decreasing  $I_D/I_G$  ratio occurred at the TC14 rGO-CNTs hybrid sample which are 0.35. This was assumed due to low  $I_D/I_G$  ratio of pristine CNTs (Kumar et al., 2013). Based on these results, the TC14 rGO-CNTs hybrid revealed lower disorder structure as compared to pristine TC14-rGO. The CNTs materials not appear high O content, thereby demonstrating small defects.

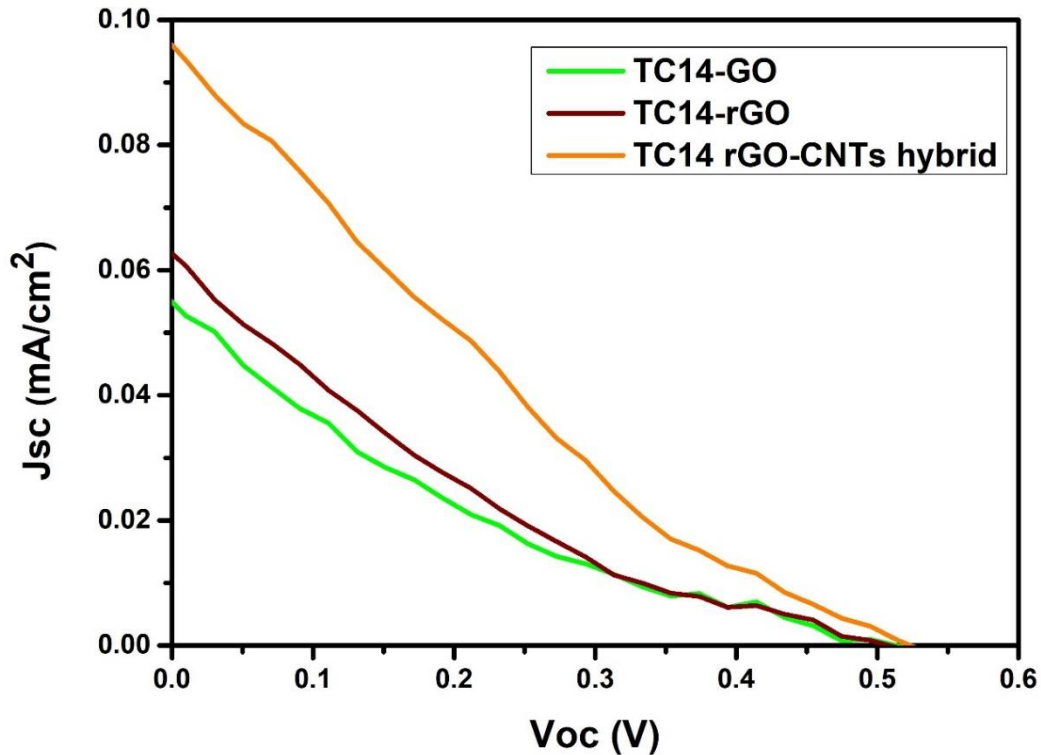


**Figure 5.** I-V Curves of TC14-GO, TC14-rGO and TC14 rGO-CNTs hybrid

Figure 5 demonstrates the electrical properties of CE samples. Higher electrical conductivity was shown by TC14-rGO of  $\sim 5.3 \times 10^{-1} \text{ S.cm}^{-1}$  as compared to TC14-GO ( $\sim 3.7 \times 10^{-1} \text{ S.cm}^{-1}$ ). Based on this result, the TC14-rGO demonstrates better conductivity than TC14-GO due to lower O content that resulted through successful reduction process (Zhao et al., 2015, Fatiatun et al., 2020). The increment of electrical conductivity occurred when TC14-rGO was hybridized with CNTs ( $\sim 6.8 \times 10^{-1} \text{ S.cm}^{-1}$ ). This was believed due to a good electrical conductivity of pristine CNTs. The details of electrical properties of TC14-GO, TC14-rGO and TC14 rGO-CNTs hybrid are shown in Table 1.

**Table 1.** Electrical properties of TC14-GO, TC14-rGO and TC14 rGO-CNTs hybrid

Samples	Resistivity, $\rho$ ( $\Omega \cdot \text{cm}$ )	Conductivity, $\sigma$ ( $\text{S} \cdot \text{cm}^{-1}$ )
TC14-GO	2.68	$3.7 \times 10^{-1}$
TC14-rGO	1.86	$5.3 \times 10^{-1}$
TC14 rGO-CNTs hybrid	1.46	$6.8 \times 10^{-1}$

**Figure 6.** *J-V* Curves of DSSCs with TC14-GO, TC14-rGO and TC14 rGO-CNTs hybrid as CE thin films

DSSCs performance can be determined by using solar simulator as shown in current density-voltage (*J-V*) curves (Figure 6). In Figure 6, the highest efficiency of DSSCs was presented by TC14 rGO-CNTs hybrid (0.0132%), followed by TC14-rGO (0.0065%) and TC14-GO (0.0560%). TC14-rGO showed higher efficiency than TC14-GO which presented the  $J_{sc}$ ,  $V_{oc}$  and  $FF$  value of 0.070  $\text{mA}/\text{cm}^2$ , 0.512 V and 0.157, respectively. The TC14-rGO demonstrated higher  $J_{sc}$  (0.070  $\text{mA}/\text{cm}^2$ ) than TC14-GO (0.055  $\text{mA}/\text{cm}^2$ ) because of higher electrical conductivity of TC14-rGO ( $\sim 5.3 \times 10^{-1} \text{ S} \cdot \text{cm}^{-1}$ ) and lower oxygen functional groups. This was assumed makes faster electron transport for the dye regeneration in DSSCs measurement thus improved DSSCs performance (Suriani et al., 2018).

Lower efficiency of TC14-GO was believed due to higher oxygen functional group which decelerated electron movement thus decreased the DSSCs performance. Meanwhile, TC14-rGO/CNTs hybrid demonstrated increasing value of  $V_{oc}$  (0.550 V),  $J_{sc}$  (0.098  $\text{mA}/\text{cm}^2$ ),  $FF$  (0.387) and efficiency of 0.0132% when compared with the pristine TC14-rGO. The conjugated network of CNTs which acted as connecting wires between the TC14-rGO layers and as filler vacancies. This offered easier electron movement thus increased the conductivity



and efficiency of TC14-rGO/CNTs hybrid CE film in DSSCs application. The summary results of  $J_{sc}$ ,  $V_{oc}$ ,  $FF$  and efficiency ( $\eta$ ) values of TC14-GO, TC14-rGO and TC14 rGO-CNTs hybrid CE thin films in DSSCs application are presented in Table 2.

**Table 2.** Summary results of  $J_{sc}$ ,  $V_{oc}$ ,  $FF$  and efficiency ( $\eta$ ) values of TC14-GO, TC14-rGO and TC14 rGO-CNTs hybrid CE thin films in DSSCs application

Types of GO-based CE	Open Circuit Voltage, $V_{oc}$ (V)	Short Circuit Current Density, $J_{sc}$ (mA/cm <sup>2</sup> )	Fill Factor, $FF$	Efficiency, $\eta$ (%)
TC14-GO	0.514	0.055	0.170	0.0052
TC14-rGO	0.512	0.070	0.157	0.0058
TC14-rGO/CNTs hybrid	0.550	0.098	0.213	0.0124

## CONCLUSION

The TC14 rGO/CNTs hybrid showed the highest efficiency of 0.0124% with  $V_{oc}$  (0.550 V),  $J_{sc}$  (0.098 mA/cm<sup>2</sup>) and  $FF$  (0.213). High efficiency of TC14 rGO/CNTs hybrid was believed due to high electrical conductivity ( $\sim 6.8 \times 10^{-1}$  S.cm<sup>-1</sup>). This was assumed makes faster electron transport for the dye regeneration in DSSCs measurement thus improved DSSCs performance. Moreover, the conjugated network of CNTs which acted as connecting wires between the TC14-rGO layers and as filler vacancies. This offered easier electron movement thus increased the efficiency of TC14-rGO/CNTs hybrid CE film in DSSCs application. This findings indicated that the TC14-rGO composited with CNTs can enhance the CE performance in DSSCs application. Therefore, this study can be utilized as basis in the next research about graphene –based CE.

## ACKNOWLEDGEMENT

This research was conducted through a novice lecturer research grant program (PDP) which was awarded through higher education (DIKTI) of the ministry of education and culture (Kemendikbud). Therefore, the researchers would like to thank the parties involved in the ministry and research, publishing, and community service institutions (LP3M) Universitas Sains Al-Qur'an so that the authors can submit proposals and get this research grant.

## REFERENCES

- Ahmed, F., Kumar, S., Arshi, N., Anwar, MS., Prakash, R. (2011). Growth and characterization of ZnO nanorods by microwave-assisted route: green chemistry approach. *Advance Material Letter*, 2(3), 183-187.
- Chadijah, S., Dahlan, D & Harmadi. (2016). Pembuatan counter electrode karbon untuk aplikasi elektroda dye-sensitized solar cell (DSSC). *Jurnal Ilmu Fisika*, 8(2), 78-86.
- Chen, X., He, D., Wu, H., Zhao, X., Zhang, J., Cheng, K., et al (2015). Platinized

- graphene/ceramics nano-sandwiched architectures and electrodes with outstanding performance for pem fuel cells. *Scientific Reports*, 5, 16246.
- Choi, H., Kim, H., Hwang, S., Han, Y., & Jeon, M. (2011). Graphene counter electrodes for dye-sensitized solar cells prepared by electrophoretic deposition. *Journal of Materials Chemistry*, 21, 7548–7551.
- Fatiatun, F., Suriani, A.B., Mohamed, A., Hashim, N., Mamat, M.H., Malek, M.F. (2017). The structural properties of ZnO/TiO<sub>2</sub> bilayer thin film as photoanode. *Sainmatika*, 14(1), 30-37.
- Fatiatun, Suriani, AB., Marwoto, P., Wibowo, KM., Muqoyyanah, & Firdaus. (2020). Effects of Various Semiconducting Oxides as Photoanode and Counter Electrode for Dye Sensitized Solar Cell Application - A Review. *Indonesian Journal of Applied Physics*, 10(2), 126-147.
- Fatiatun, Firdaus, Jumini, S., Suriani AB., Marwoto, P., Wibowo, KM., Astuti B. (2020). Enhanced electrical conductivity of counter electrode using hybrid of reduced graphene oxide assisted with customised triple-tail surfactant with multiwalled carbon nanotubes. *Journal of Physics: Conference Series*, 1517. 012059 1-7.
- Grätzel, M. (2003). Dye-sensitized solar cells. *Journal of Photochemistry and Photobiology C: Photochemistry Reviews*, 4(2), 145–153.
- Ichikawa, Y., Yoshida, T., Hama, T., Sakai, H., Harashima, K. 2001. Production technology for amorphous silicon-based flexible solar cells. *Solar Energy Materials & Solar Cells*, 66, 107-115.
- Idris, NJ., Suriani, AB., Muqoyyanah, Mohamat R., Fatiatun, Ahmad, MK. (2019). Fabrication of sand/zinc oxide/titanium dioxide nanocomposite as photocatalyst. *SPEKTRA: Jurnal Kajian Pendidikan Sains*, 5(2), 122-128.
- Kumar, K., Kim, Y., Li, X., Ding, J., Fisher, F. T., Yang, E., et al (2013). Chemical vapor deposition of carbon nanotubes on monolayer graphene substrates: reduced etching via suppressed catalytic hydrogenation using C<sub>2</sub>H<sub>4</sub>. *Chemistry of Materials*, 25(19), 3874-3879.
- Marwoto, P., Fatiatun., Sulhadi., Sugianto., & Aryanto, D. (2016). Effects of argon pressure on the properties of ZnO:Ga thin film deposited by DC magnetron sputtering. *AIP Conference Proceedings*, 1719, 030016 1-6.
- Samad, NAA., Lai, CW., Lau, KS, Hamid, SBA. (2016). Efficient Solar-Induced Photoelectrochemical Response Using Coupling Semiconductor TiO<sub>2</sub>-ZnO Nanorod Film. *Materials*, 9(937), 1-21.
- Sulhadi, Fatiatun, F., Marwoto, P., Sugianto, Wibowo, E. (2015). Deposition temperature variations on the structure, optical and electrical properties of zinc oxide thin films doped gallium (ZnO:Ga). *Jurnal Pendidikan. Fisika Indonesia*, 11(1), 93-99.
- Suriani, A. B., Fatiatun, Mohmed, A., Muqoyyanah., Hashim, N., Rosmi, M.S., Mamat, M.H., Malek, M.F., Salifairus, M.J., Khalil, H.P.S.A. 2018. Reduced graphene oxide/platinum hybrid counter electrode assisted by custom-made triple-tail surfactant and zinc oxide/titanium dioxide bilayer nanocomposite photoanode for enhancement of DSSCs photovoltaic performance. *Optik*, 161, 70–83.

- Suriani, A.B., Muqoyyanah, Mohamed, A., Mamat, MH., Hashim, N., Isa I, Malek, MF, Kairi, MI, Mohamed, AR, Ahmad, MK. (2018). Improving the photovoltaic performance of DSSCs using a combination of mixed-phase TiO<sub>2</sub> nanostructure photoanode and agglomerated free reduced graphene oxide counter electrode assisted with hyperbranched surfactant. *Optik*, 158, 522-534.
- Suriani. A. B., Fatiatun, Mohamed, A., Muqoyyanah., Hashim, N., Mamat, M.H., Ahmad, M.K., Marwoto, P. 2019. Improved DSSC photovoltaic performance using reduced graphene oxide–carbon nanotube/platinum assisted with customised triple - tail surfactant as counter electrode and zinc oxide nanowire/titanium dioxide nanoparticle bilayer nanocomposite as photoanode. *Graphene Technol*, 4, 17-31.
- Suriani, A.B., Muqoyyanah, Mohamed, A., Mamat, MH., Othman, MHD., Ahmad, MK., Khalil, HPSA., Marwoto, P., Birowosuto, MD. (2019). Titanium dioxide/agglomerated-free reduced graphene oxide hybrid photoanode film for dye sensitized solar cells photovoltaic performance improvement. *Nano-Structures & Nano-Objects*, 18, 100314 1-100314 14.
- Wu, M & Ma T. (2014). Recent progress of counter electrode catalysts in dye sensitized solar cells. *The Journal of Physical Chemistry C*, 118(30), 16727-16742.
- Yang, Z., Chen, T., He, R., Guan, G., Li, H., Qiu, L., & Peng, H. (2011). Aligned carbon nanotube sheets for the electrodes of organic solar cells. *Advanced Materials*, 23(45), 5436–5439.
- Yadav, R. R., Rout, C. S., & Moshkalev, S. A. (2017). Synthesis of self-assembled and hierarchical palladium-CNTs reduced graphene oxide composites for enhanced field emission properties. *Materials & Design*, 122, 110-117.
- Zhao, J., Liu, L., Li, F. (2015). Graphene oxide: Physics and applications. *Springer*, 31-56.